J. Biochem. 2010;148(1):55–69 doi:10.1093/jb/mvq033

JB THE JOURNAL OF BIOCHEMISTRY

Anti-human HB-EGF monoclonal antibodies inhibiting ectodomain shedding of HB-EGF and diphtheria toxin binding

Received January 8, 2010; accepted March 19, 2010; published online March 23, 2010

Miki Hamaoka[1,†], Ichino Chinen[1,†], Takuya Murata[2], Seiji Takashima[3], Ryo Iwamoto[1] and Eisuke Mekada[1,*]

[1]Department of Cell Biology, Research Institute for Microbial Diseases, Osaka University, 3-1, Yamadaoka, Suita, Osaka 565-0871, [2]Obstetrics and Gynecology, Osaka Saiseikai Nakatsu Hospital, 2-10-39, Matta, Kitaku, Osaka 530-0012 and [3]Department of Molecular Cardiology, Osaka University Graduate School of Medicine, 2-2 Yamadaoka, Suita, Osaka 565-0871, Japan

*Eisuke Mekada, Department of Cell Biology, Research Institute for Microbial Diseases, Osaka University, 3-1, Yamadaoka, Suita, Osaka 565-0871, Japan. Tel: +81 6 6879 8286, Fax: +81 6 6879 8289, email: emekada@biken.osaka-u.ac.jp

†These authors contributed equally to this work.

HB-EGF is a member of the EGF family of growth factors that bind and activate the EGF receptor. HB-EGF is synthesized as a membrane-anchored protein (proHB-EGF), and then proteolytically cleaved, resulting in the mitogenically active soluble form. ProHB-EGF functions as the receptor for the diphtheria toxin (DT). HB-EGF plays pivotal roles in pathophysiological processes, including cancer. Monoclonal antibodies (mAbs) specific for HB-EGF could be an important tool in HB-EGF research. However, few such mAbs have been established to date. In this study, we newly generated seven clones of hybridoma-derived mAbs by immunizing HB-EGF null mice with recombinant human HB-EGF protein. All mAbs specifically bound to human HB-EGF but not to mouse HB-EGF. Epitope mapping analysis showed that most of the mAbs recognized the EGF-like domain. Although none of the newly isolated mAbs directly inhibited the mitogenic activity of HB-EGF for EGFR-expressing cells, some strongly inhibited DT-binding. Interestingly, some of the mAbs efficiently inhibited ectodomain shedding of proHB-EGF, and consequently prevented the cell growth of the EGFR-expressing cells in a co-culture system with proHB-EGF-expressing cells. Hence, these new anti-HB-EGF mAbs may advance clinical as well as basic research on HB-EGF.

Keywords: ectodomain shedding/EGF receptor/epitope mapping/growth inhibition/HB-EGF.

Abbreviations: DT, diphtheria toxin; EGFR, EGF receptor; HB-EGF, heparin-binding EGF-like growth factor; LPA, lysophosphatidic acid; mAb, monoclonal antibody; pAb, polyclonal antibody; rhHB-EGF, recombinant human HB-EGF; sHB-EGF, soluble form of HB-EGF; TPA, 12-*O*-tetradecanoylphorbol-13-acetate.

Heparin-binding EGF-like growth factor (HB-EGF) is a member of the EGF family of growth factors that bind and activate the EGF receptor (EGFR) and ErbB4 (*1*, *2*). Like other members of the EGF family, HB-EGF is synthesized as a membrane-anchored protein (proHB-EGF), composed of a signal peptide, propeptide, heparin-binding, EGF-like, juxtamembrane, transmembrane and cytoplasmic domains (*3*). ProHB-EGF is biologically active as a juxtacrine growth factor that signals to neighbouring cells in a non-diffusible manner (*4*, *5*), and also functions as the receptor for the diphtheria toxin (DT) (*6*, *7*). ProHB-EGF is cleaved at its juxtamembrane domain by metalloproteases in a process called ectodomain shedding (*8*). Ectodomain shedding of proHB-EGF yields a soluble form of HB-EGF (sHB-EGF), which is a potent mitogen and chemoattractant for cells expressing its cognate ErbB receptor (*9*).

Recent studies using genetically engineered HB-EGF mutant mice have revealed that HB-EGF is involved in a number of physiological processes *in vivo* (*10*), including proper heart development and function (*11–14*), eyelid closure (*15*), skin wound healing (*16*), retinoid-induced skin hyperplasia (*17*), blastocyst implantation (*18*) and lung development (*13*, *19*). Furthermore, HB-EGF is also involved in a number of pathological processes, including cardiac hypertrophy (*20*), smooth muscle cell hyperplasia (*21*), pulmonary hypertension (*22*), oncogenic transformation (*23*) and tumorigenesis in ovarian cancer (*24*, *25*).

Monoclonal antibodies (mAbs) specific for HB-EGF are an important tool in HB-EGF research, but few such mAbs have been established to date. In this study, we newly generated seven clones of hybridoma-derived mAbs, mapped epitopes of these antibodies in a HB-EGF molecule, and characterized the availability of these mAbs for several research applications. We also show that some of the mAbs inhibit the ectodomain shedding of proHB-EGF, suggesting that these mAbs could be used as a HB-EGF-specific ectodomain shedding inhibitor.

Materials and Methods

Materials

12-*O*-tetradecanoylphorbol-13-acetate (TPA) and rabbit anti-FLAG polyclonal antibody were purchased from Sigma-Aldrich. Lysophosphatidic acid (LPA) was purchased from Funakoshi Co. Ltd. Anisomycin was purchased from Nacalai. Mouse anti-human HB-EGF MAB259, recombinant human HB-EGF (rhHB-EGF), and recombinant mouse IL-3 were obtained from R&D systems. Rabbit anti-HA polyclonal antibody, goat anti-human HB-EGF polyclonal antibody (pAb) C-18 and goat anti-mouse HB-EGF pAb M-18 were obtained from Santa Cruz Biotechnology Inc. Rabbit anti-human HB-EGF antibody H-6 was produced as described previously (*6*). DT was prepared as described previously (*26*).

Preparation of anti-human HB-EGF mAbs

The recombinant ectodomain of human HB-EGF antigen for immunization was prepared by the baculovirus expression system. Mouse anti-human HB-EGF ectodomain mAbs were prepared by immunizing HB-EGF null mice (*12*) with an abdominal injection of the recombinant ectodomain of the human HB-EGF antigen. Preparation and cloning of hybridomas producing an antibody reacting to human HB-EGF was performed by ELISA screening by Medical and Biological Laboratories Co. Ltd. The immunoglobulin isotype of the antibody was determined by ImmunoPure Monoclonal Antibody Isotyping Kit I (Pierce) according to the manufacturer's instructions. The IgG fraction of the conditioned medium of the cloned hybridoma was purified by Protein A affinity chromatography.

Plasmids

Expression vectors encoding human/mouse HB-EGF chimeras (Fig. 3A) and human HB-EGF mutants with a point mutation in EGF-like domain (Fig. 4A) were prepared as described previously (*27*, *28*).

Cell culture and transfection

Vero, Vero-H (Vero stably expressing human HB-EGF) (*8*) and Vero-mH (Vero stably expressing mouse HB-EGF) (*14*) cells were maintained in modified Eagle's medium (MEM) with non-essential amino acids (MEM-NEAA) supplemented with heat-inactivated 10% fetal calf serum (FCS). Vero cells expressing C-terminally FLAG-tagged HB-EGF (Vero-H-FLAG), HA-tagged HB-EGF (Vero-H-HA), HA-tagged TGFα (Vero-TGF-HA), HA-tagged epiregulin (Vero-EPR-HA), HA-tagged betacellulin (Vero-BTC-HA) and HA-tagged amphiregulin (Vero-AR-HA) were prepared as previously described (*29*). Mouse L cells were maintained in DMEM with 10% FCS. DER cells (*5*), 32D cells that stably express EGFR, were grown in RPMI 1640 medium containing 10% FCS and 1 ng/ml IL-3. Transfection of the cells was carried out with plasmids by the calcium–phosphate method as described previously (*6*).

Cell binding assay

Cells (5×10^4 or 1×10^5) in 48- or 24-well multiplates, respectively, were incubated with each mAb at the indicated concentrations, or with H-6 rabbit pAb (2 μg/ml) in the binding medium (Ham's F12 medium buffered with 20 mM HEPES–NaOH, pH 7.2, containing 10% FCS) for 2 h at 4°C. Cells were then washed twice with washing buffer [1 mg/ml BSA-containing PBS(+) (PBS with 0.5 mM $CaCl_2$ and 0.5 mM $MgCl_2$)] and once with PBS(+), and fixed with 1.75% formaldehyde in PBS(+) for 20 min at 4°C. After washing once with PBS(+), fixed cells were blocked with blocking solution (0.2 M Glycine, 0.1 M Tris–HCl, pH 8.1) for 30 min at 4°C. After incubation with washing buffer for 20 min at 4°C, cells were incubated with HRP-conjugated anti-mouse IgG Ab (Chemicon). In the case of H-6 binding, HRP-conjugated anti-rabbit IgG Ab was used as a secondary antibody. After washing twice with washing buffer and twice with PBS(+), colour development detection was carried out by POD reagent (Nakalai) according to the manufacturer's instructions. Light emission was measured at 450 nm using a microplate reader (Thermo Electron Corp.).

Epitope mapping

For detection of the domains in human HB-EGF that are recognized by the mAbs, L cells that were transfected with a series of the expression vector encoding human/mouse HB-EGF chimeras (Fig. 3A) were tested by cell binding assay as described above. For detection of the amino acid residues in the EGF-like domain in human HB-EGF that are recognized by the mAbs, L cells that were transfected with a series of the expression vector encoding human HB-EGF mutants with a point mutation in EGF-like domain (Fig. 4A) were tested by cell binding assay as described above. The score of the binding of each mAb to HB-EGF mutant molecules on the cell surface was normalized with the binding of H-6 pAb, as a standard for the expression of each construct.

Immunoblotting

For immunoblot analysis, cells were lysed with cell lysis buffer [60 mM 1-*O*-n-octyl-β-D-glucopyranoside, 0.15 M NaCl, 10 mM HEPES–NaOH, pH 7.2, 1/100× protease inhibitor cocktail (Nacalai)], and centrifuged at 20,000× *g* for 30 min. The supernatant was collected, mixed with SDS gel sample buffer, and loaded onto 15% SDS gel electrophoresis gels. Separated proteins were electro-transferred to a polyvinylidene difluoride membrane (Immobilon-P, Millipore), and the transferred membrane was blocked in TTBS (10 mM Tris–HCl pH 7.5, 0.15 M NaCl, 0.05% Tween20) containing 1% skim milk for 1 h, followed by incubation with a primary antibody in TTBS containing 1% skim milk for 1 h. After washing the membrane with TTBS, it was incubated with HRP-conjugated a cognate secondary antibody (1:3,000) for 1 h. The membrane was washed with TTBS, and chemiluminescent detection was carried out with the ECL detection system (Pierce) according to the manufacturer's instruction.

Immunoprecipitation

Cell surface biotinylation and immunoprecipitation of HB-EGF were performed as described previously (*6*). In brief, Vero or Vero-H cells were labelled with a biotinylation reagent, sulpho-NHS-biotin (Perbio Science). Surface-biotinylated cells were homogenized in cell lysis buffer, and the lysate was used for immunoprecipitation with each mAb (2 or 0.1 μg/ml) and sepharose-conjugated anti-mouse IgG. The precipitated proteins were analysed by SDS–PAGE and western blotting using HRP-conjugated streptavidin (Perbio Science).

Immunohistochemistry for human cervical cancer tissues

Invasive cervical squamous cell carcinoma tissue was prepared from a cervical cancer patient. The patient was operated at the Osaka University hospital. Informed consent was obtained for the clinical sample. Acquisition of the tissue was approved by the local ethical committee. Surgically removed tissue was sampled for histological diagnosis and the remainder was cut down. Unfixed tissue was directly embedded into Tissue-Tek OCT Compound (Sakura Finetechnical Co. Ltd.), which was used for the frozen tissue section. Four-micrometer sections were fixed with chilled acetone for 10 min. The endogenous hydrogen peroxidase was quenched with 0.03% H_2O_2 in methanol for 10 min. Sections were incubated with each mAb at 10 μg/ml in blocking solution Block Ace (Dainihon Seiyaku) overnight at 4°C, and then incubated with biotinylated goat anti-mouse secondary antibody (Vector laboratories) diluted 1:200 for 1 h at room temperature. Staining was developed using a R.T.U. Vectastain kit (Vector laboratories) and a diaminobenzidine (DAB) substrate (Merck). Sections were counterstained lightly with haematoxylin.

Neutralization assay for HB-EGF growth factor activity

HB-EGF mitogenic assay was performed as previously described (*30*). In brief, DER cells (1×10^4 cells/well of a 24-well multiplate) were incubated with 10 ng/ml of rhHB-EGF in the presence or absence of 10 μg/ml heparin, and the presence of various concentrations of each mAb, CRM197, or anti-HB-EGF neutralizing pAb, for 42 h at 37°C. The number of DER cells was then measured by cell count reagent (Nakalai) according to the manufacturer's instructions.

DT binding assay

Binding of ^{125}I-labelled DT to the Vero-H cells in the presence of various concentrations of each mAb was measured as described previously (*30*). Briefly, Vero-H cells (1×10^5 cells/well of a 24-well multiplate) were incubated with ^{125}I-DT (50 ng/ml) in the presence of indicated concentrations of each mAb for 12 h at 4°C. Then, cells were lysed with 0.1 N NaOH, and the radioactivity was measured with a γ-counter. Non-specific binding of ^{125}I-DT was assessed in the presence of a 1,000-fold excess of unlabelled DT. Specific binding was determined by subtracting the non-specific binding from the total binding obtained with ^{125}I-DT alone.

HB-EGF shedding assay

Ectodomain shedding assay of HB-EGF was performed as previously described (*29*) unless otherwise stated. Briefly, Vero-H-FLAG cells (1×10^6 cells/60 mm dish) were serum-starved for 4 h and pre-incubated with 10 μg/ml of each mAb or CRM197 at 37°C for 30 min. Following treatment with TPA (64 nM), LPA (10 μg/ml), or anisomycin (10 μg/ml) for 30 min, cells were lysed with cell lysis buffer, and the lysates were subjected to immunoblotting. Ectodomain shedding of HB-EGF was monitored by generation of the C-terminal fragment, using an anti-FLAG antibody for FLAG-tagged HB-EGF. Ectodomain shedding of mouse HB-EGF was carried out by using Vero-mH cells, and monitored by using anti-C-terminal fragment of mouse HB-EGF (M-18). Ectodomain shedding of HA-tagged HB-EGF, TGFα and EPR was carried out by using Vero-H-HA, Vero-TGF-HA and Vero-EPR-HA cells, and monitored by using anti-HA antibody. Quantification of the extent of shedding was performed by densitometry, and calculated as the ratio of the density of the C-terminal fragment to that of the total band.

Co-culture assay

Vero-H cells were placed in 24-well multiplates at a density of 1×10^5 cells/well and cultured in MEN-NEAA containing 10 μg/ml heparin overnight. The cells were washed twice with RPMI1640 containing 10 μg/ml heparin, and Transwell (0.4-μm pore size, Millipore Corp) were introduced onto the Vero-H cells in the well. Then DER cells were added to the Transwell at 2×10^4 cells/well, followed by incubation in RPMI1640 containing 10% FCS, 10 μg/ml heparin, and 10 μg/ml of each mAb, anti-HB-EGF neutralizing pAb or CRM197. After co-culture for 48 h, DER cells were harvested from the Transwell, and the cell number was measured as described above.

Results

Production of mouse anti-human HB-EGF mAbs by immunizing HB-EGF null mice

Despite longstanding efforts, we did not obtain mAbs against HB-EGF. A few clones are commercially available for anti-HB-EGF mAb to date. Considering the difficulty to obtain mAbs against HB-EGF by immunizing normal mice, we carried out immunization with a recombinant human HB-EGF protein in HB-EGF null mice, from which anti-HB-EGF mAbs-producing hybridoma clones were expected to be isolated more easily. As a result, we obtained a total seven clones of hybridomas producing IgGs that recognize the HB-EGF antigen (Table I). We characterized these seven clones of anti-human HB-EGF mAbs for several applications. In this study, MAB259, a commercially available anti-HB-EGF mAb, was used as a standard mAb for evaluation of our newly prepared mAbs.

Binding specificity of mAbs to HB-EGF expressed on the cell surface

First we characterized the binding specificity of mAbs for HB-EGF among EGF family growth factors. For this purpose, antibody binding assays were performed using Vero, Vero-H-HA, Vero-TGF-HA, Vero-EPR-HA and Vero-BTC-HA cells. All seven mAbs and MAB259 showed specific binding to Vero-H-HA cells, but not to the other cells (Fig. 1A and B). Binding assay was also performed in Vero-AR-HA cells. Although the expression of HA-tagged AR in Vero-AR-HA cells was low, the result indicated that none of the mAbs showed any binding to Vero-AR-HA cells (Fig. 1C). Vero cells express monkey HB-EGF endogenously, but the specific binding of the obtained mAbs or MAB259 was not detected by this assay. We suspect this was because of the low expression level, rather than amino acid variations between

Table I. Summary of anti-human HB-EGF mAbs characterization

Ab name	Isotype	Epitope		Applications							
		Domain	Amino acid	ICC[a]	WB[b]	IP	IHC	Neut/GF/DER	Neut/DTR	Shedding inhibition	Suitable applications for
4G10	IgG1	EGF	E141	++	++	+++	−	−	+++	+++	ICC, WB, IP
3H4	IgG1	EGF	E141	++	++	+++	−	−	(n.d.)	+++	ICC, WB, IP
1F3	IgG1	EGF	E141	++	+	+	−	−	+++	+++	ICC
5D9	IgG2a	EGF	E141	+	−	+++	+	−	+++	++	IP, IHC
7E10	IgG1	EGF	I133/H135	++	−	+	−	−	+++	++	ICC
3D9	IgG1	EGF	I133/H135	++	−	+	−	−	(n.d.)	(n.d.)	ICC
6C11	IgG2a	HB	(n.d.)	+	−	++	+[c]	−	(n.d.)	+	IHC
MAB259	IgG2a	EGF	H135	+	+	++	+	+	+	+	IHC

In all characterization experiments, all mAbs reacted with human HB-EGF, but not with mouse HB-EGF. Suitability of each mAb for each application is indicated as a relative value among all mAbs: −, negative; +, positive; ++, strongly positive; +++, extremely positive; ICC, immunocytochemistry; WB, western blotting; IP, immunoprecipitation; IHC, immunohistochemistry; Neut/GF/DER, neutralization of HB-EGF growth factor activity in DER assay; Neut/DTR, neutralization of DTR activity; Shedding inhibition, inhibition of HB-EGF ectodomain shedding.

[a]Availability of these mAbs for ICC was quantitatively evaluated by binding-ELISA assay to HB-EGF expressed on the cell surface.

[b]These mAbs are available for WB under non-reducing conditions.

[c]Availability of these mAbs for IHC was tested by using conditioned media of the hybridoma, but not by using purified IgG (data not shown).

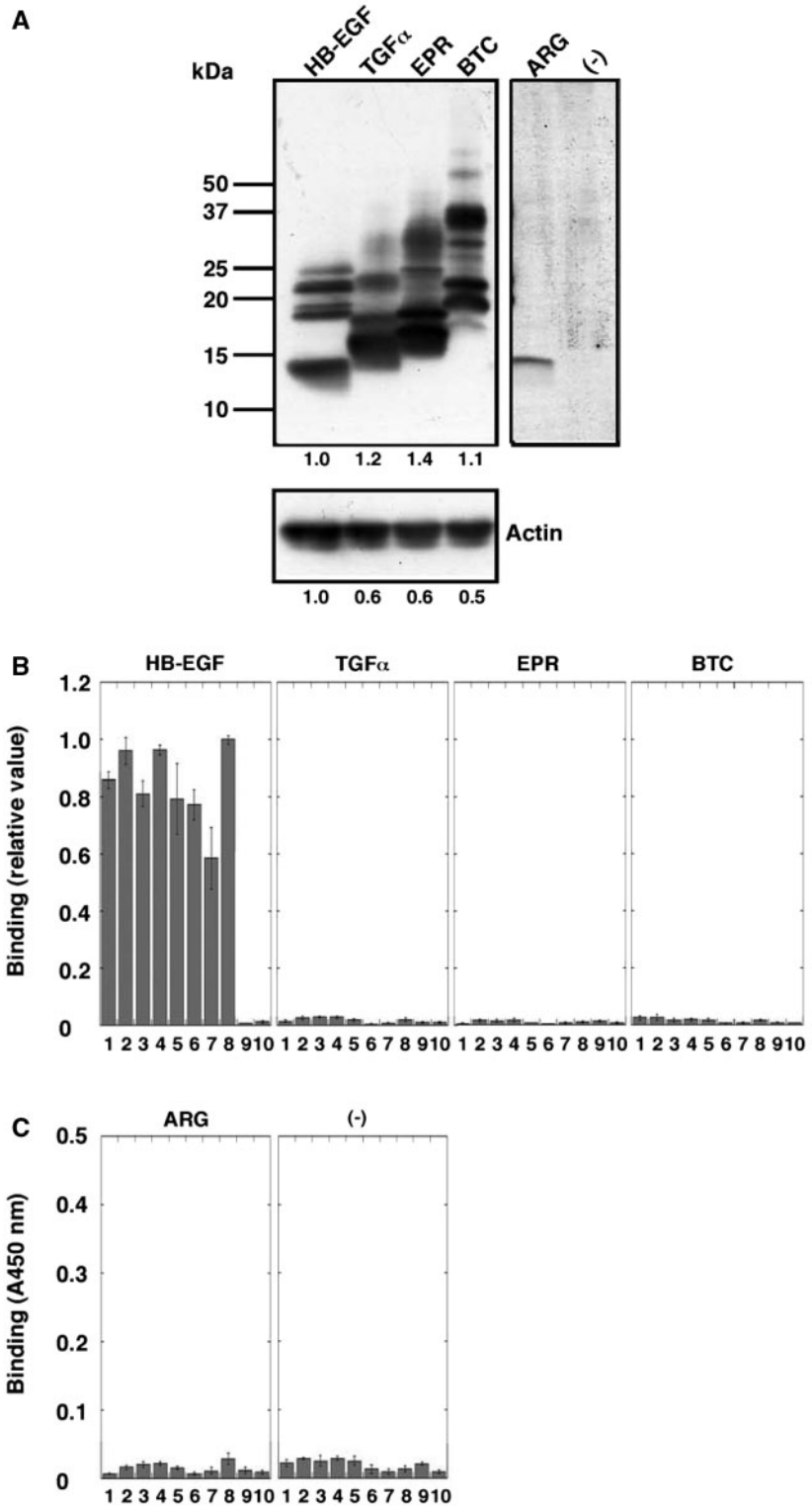

Fig. 1 Specific binding of anti-human HB-EGF mAbs to HB-EGF among EGFR ligands. (A) Expression levels of HA-tagged HB-EGF, TGFα, EPR, BTC and ARG in Vero-H-HA cells, Vero-TGF-HA cells, Vero-EPR-HA cells, Vero-BTC-HA cells and Vero-ARG-HA cells, respectively, were determined by immunoblotting probed by an anti-HA antibody. Density of each HA-band was normalized with that of the corresponding actin-band, except for the case of ARG. Scores of relative density are indicated below each blotting panel. (B) Relative binding of anti-human HB-EGF mAbs to HA-tagged EGFR ligands expressed in Vero-H-HA cells, Vero-TGF-HA cells, Vero-EPR-HA cells and Vero-BTC-HA cells. Cells were incubated with 1 μg/ml of each mAb (1, 1F3; 2, 4G10; 3, 5D9; 4, 3H4; 5, 7E10; 6, 3D9; 7, 6C11; 8, MAB259; 9, anti-Myc mAb for control; 10, without mAb). Binding of the mAbs was measured by cell binding ELISA assay as described in the 'Materials and Methods' section. The relative binding value was normalized with each expression level of the HA-tagged growth factor determined by immunoblotting using an anti-HA antibody [as shown in (A)], and expressed as a ratio of the binding of MAB259 to Vero-H-HA cells. Each bar indicates the mean ± SE ($n = 3$). (C) Binding of anti-human HB-EGF mAbs to Vero-ARG-HA cells and Vero cells. Cells were incubated with 1 μg/ml of each mAb (1, 1F3; 2, 4G10; 3, 5D9; 4, 3H4; 5, 7E10; 6, 3D9; 7, 6C11; 8, MAB259; 9, anti-Myc mAb for control; 10, without mAb). Binding of the mAbs was measured by cell binding ELISA assay and the results are shown in chromogen concentration measured by absorbance of 450 nm. Each bar indicates the mean ± SE ($n = 3$).

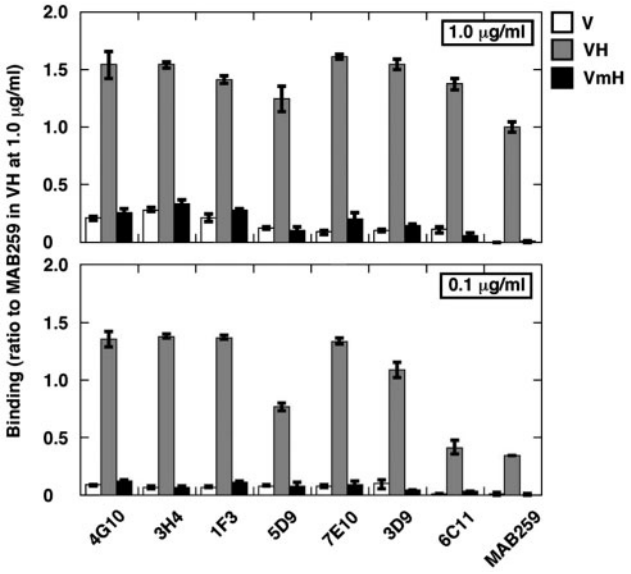

Fig. 2 Binding of anti-HB-EGF mAbs to cells overexpressing mouse HB-EGF or human HB-EGF on the cell surface. Vero cells (V), Vero-H cells (VH) or Vero-mH cells (VmH) were incubated with mAb at the concentration of 1.0 μg/ml (upper panel) or 0.1 μg/ml (lower panel). Binding of mAbs was measured by ELISA assay as described in the 'Materials and Methods' section. The relative binding value is expressed as a ratio to the binding of MAB259 to Vero-H cells at the mAb concentration of 1.0 μg/ml. Each bar indicates the mean ± SE ($n = 3$).

human and monkey HB-EGF (*7*). These results indicate that all obtained mAbs recognized HB-EGF but not other EGF family growth factors, although binding assays of mAbs to EGF were not performed.

Then we characterized the species specificity of the reactivity of mAbs to HB-EGF. For this purpose, antibody binding assays were performed using Vero, Vero-H and Vero-mH cells. All seven mAbs and MAB259 showed specific binding to Vero-H cells, but not to Vero-mH cells at the antibody concentration of 1 μg/ml (Fig. 2, upper graph), indicating that all obtained mAbs recognize human HB-EGF, but not mouse HB-EGF. Binding assays were also performed at a lower concentration of mAbs (0.1 μg/ml) to roughly estimate the binding affinity of each mAb (Fig. 2, lower graph). Among the seven mAb clones, 4G10, 3H4, 1F3, 7E10 and 3D9 exhibited strong binding to Vero-H cells compared with MAB259 and the other mAb clones isolated in this study. Thus, these five mAbs are suitable for detection of cell surface expression of human HB-EGF by immunofluorescence or antibody-binding assay using primary or secondary labelled antibodies.

Epitope mapping

In the cell binding assay, all mAbs bound to human HB-EGF, but not to mouse HB-EGF. Taking advantage of the species specificity, we determined the epitope region of the human HB-EGF molecule for each mAb. A series of human/mouse HB-EGF chimeric molecules (Fig. 3A) (*27*) were expressed by mouse L cells, then cell binding assays were performed. As shown in Fig. 3B, 4G10, 3H4, 1F3 and 5D9 bound to only H (1–186)-expressing cells, while 7E10, 3D9 and MAB259 bound to both H (1–186)-expressing and H (1–136)-expressing cells. 6C11 bound to H (1–186)-expressing, H (1–136)-expressing and H (1–106)-expressing cells. Thus, considering that the antigen used for immunization covered amino acid residues 23–149 of HB-EGF, 4G10, 3H4, 1F3 and 5D9 bind to the site between amino acids residues 136–149 of the EGF-like domain, and 7E10, 3D9 and MAB259 bind to the site between amino acids residues 106–136 of the EGF-like domain. In addition, 6C11 recognizes domains upstream from the EGF-like domain of human HB-EGF, which contains the heparin-binding domain (Fig. 3C).

In order to narrow down the epitope of each mAb that recognizes the EGF-like domain, we performed binding assays to L cells expressing 10 independent single mutants of HB-EGF. There are 10 amino acid differences between the EGF-like domain of human HB-EGF and that of mouse HB-EGF. We made 10 independent mutants, replacing a single amino acid within the EGF-like domain of human HB-EGF with the corresponding amino acid residue in mouse HB-EGF (Fig. 4A) (*28*). The mutant proteins were expressed in L cells, and cell binding assays were performed. As shown in Fig. 4B, 4G10, 3H4, 1F3 and 5D9 did not bind to E141H, while 7E10 and 3D9 did not bind to I133K and H135L. MAB259 did not bind to H135L. 6C11 bound to all constructs. These results are quite consistent with the results of the domain-mapping analyses determined by human/mouse chimera.

Thus, among the seven new mAbs and MAB259 tested, one clone recognizes a region upstream EGF-like domain (6C11: upstream-group; here named the epitope group), four clones recognize the region containing E141 (4G10, 3H4, 1F3 and 5D9: E141-group), one clone recognizes the region containing H135 (MAB259: H135-group), and two clones recognize the region containing both I133 and H135 (7E10 and 3D9: I133/H135-group) in the EGF-like domain. Result of the epitope mapping is summarized in Fig. 4C.

Applicability to various immunoassays

The applicability of each mAb for immunoblotting was examined. Cell lysates of Vero, Vero-H and Vero-mH cells were subjected to SDS–PAGE without reducing reagents and immunoblotting with each mAb. As shown in Fig. 5A, mAbs 3H4, 1F3, and 4G10 and MAB259 could detect human HB-EGF expression in Vero-H cells, while the other mAbs could not detect HB-EGF by immunoblotting (data not shown). Reactivity of 3H4 and 4G10 was stronger than that of 1F3 and MAB259. These mAbs failed to detect human HB-EGF in the sample subjected to SDS–PAGE in the presence of 10% β-mercaptoethanol (data not shown). M-18, anti-mouse HB-EGF pAb, detected both human and mouse HB-EGF, but none of the mAbs tested in this study detected mouse HB-EGF by immunoblotting.

To examine the applicability for immunoprecipitation, cell surfaces of Vero and Vero-H cells were

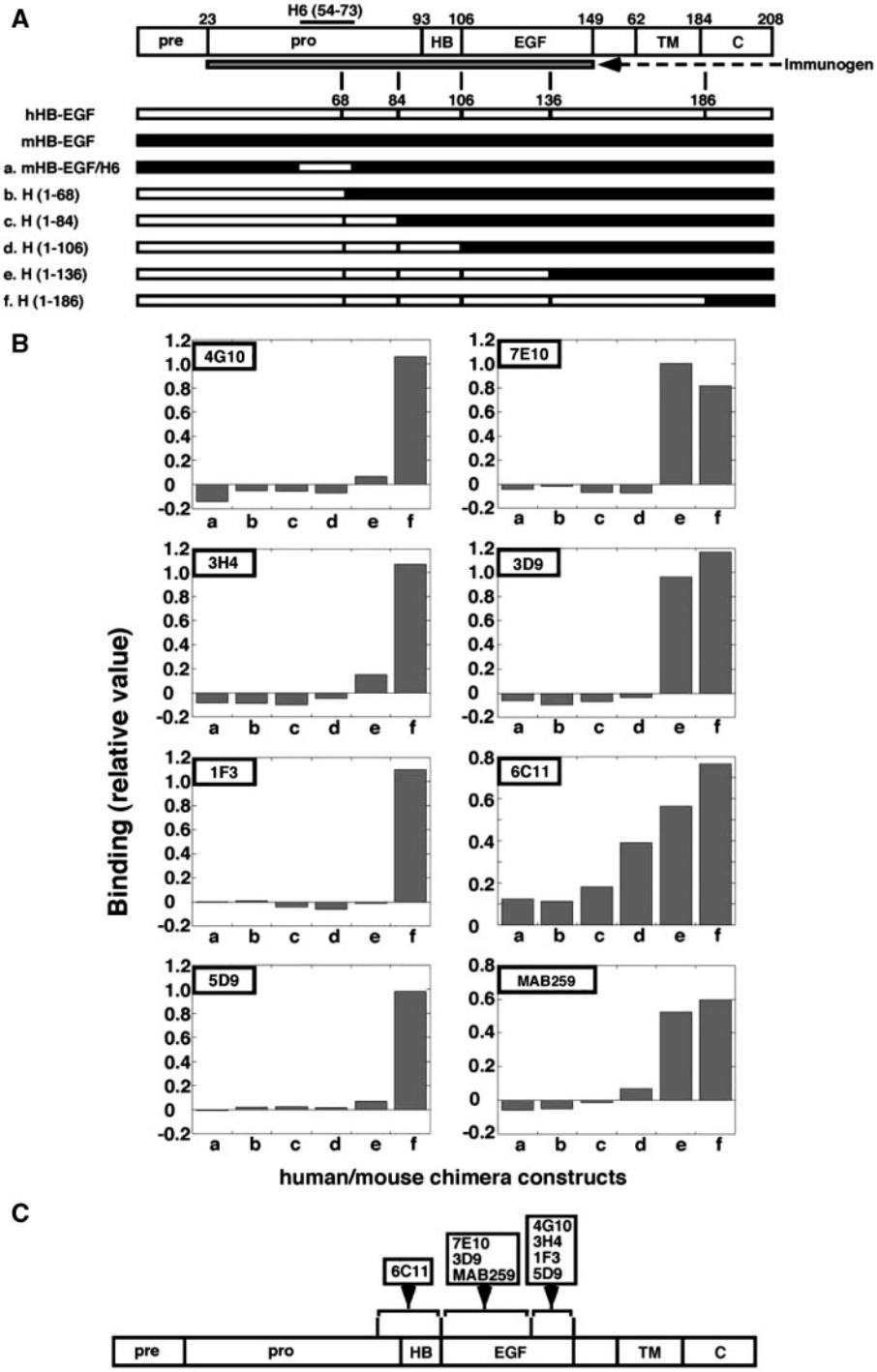

Fig. 3 Epitope mapping of each mAb using human–mouse chimeric forms of HB-EGF. (A) Schematic structures of the human/mouse HB-EGF chimeras. (B) Binding of each mAb to the L cells expressing human/mouse HB-EGF chimeric constructs as shown in (A): a, mHB-EGF/H6-tag; b, H (1–68); c, H (1–84); d, H (1–106); e, H (1–136); f, H (1–186). Binding of mAbs was measured by cell binding ELISA assay as described in the 'Materials and Methods' section. The relative binding value in each graph represents data that is normalized with the binding of H-6 pAb, which binds to all constructs, to the cells. (C) Summary of the results shown in (B).

labelled with the membrane-impermeable biotinylation reagent sulpho-NHS-biotin. Then they were lysed, and the lysate was precipitated by each mAb followed by SDS–PAGE and immunoblotting with HRP-conjugated streptavidin. As shown in Fig. 5B-a, all seven mAbs precipitated human HB-EGF in various degrees of precipitating activity. Among all tested mAbs, 4G10, 3H4 and 5D9 had the strongest precipitation activity, even at the concentration of 0.1 μg/ml (Fig. 5B-b). None of the seven mAbs precipitated mouse HB-EGF in Vero-mH cells (data not shown).

Next we tested the applicability of mAbs for immunohistochemistry of frozen sections of human cervical cancer (Fig. 6A). Among the seven new mAbs and

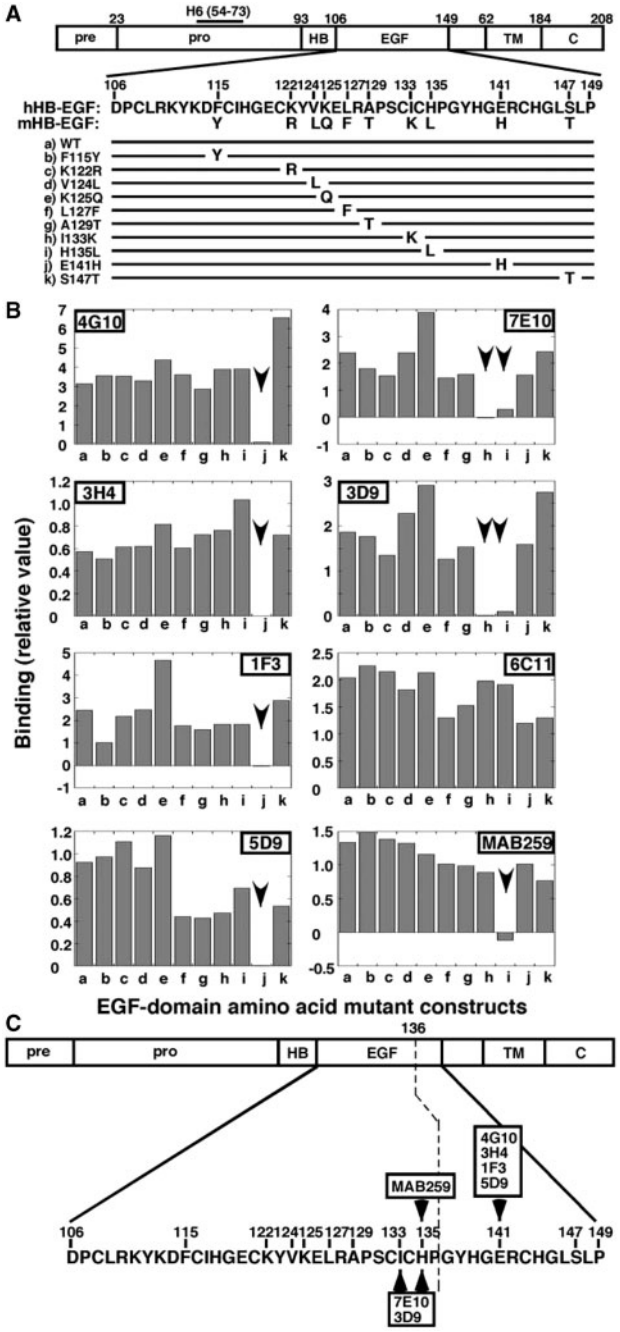

Fig. 4 Epitope mapping of each mAb using point mutants in the EGF-like domain of human HB-EGF. (A) Schematic structures of the human HB-EGF mutants. (B) Binding of each mAb to the L cells expressing each human HB-EGF mutant construct as shown in (A): a, WT human HB-EGF; b, F115Y; c, K122R; d, V124L; e, K125Q; f, L127F; g, A129T; h, I133K; i, H135L; j, E141H; k, S147T. Binding of mAbs was measured by cell binding ELISA assay as described in the 'Materials and Methods' section. The relative binding value in each graph represents data that is normalized with the binding of H-6 pAb, which binds to all constructs, to the cells. (C) Summary of the results shown in (B).

MAB259, 5D9 and MAB259 gave the best results for immunohistochemistry. 5D9 (Fig. 6B) and MAB259 (data not shown) displayed representative staining for HB-EGF in the tumour area (Fig. 6b), but not in the surrounding normal peripheral area (Fig. 6c). In human cervical cancer, HB-EGF is predominantly expressed in the cancer-associated stroma region (Murata, unpublished observation). Consistently, signals of HB-EGF by 5D9 predominantly appeared in the stromal regions (Fig. 6B-b).

Neutralization of HB-EGF mitogenic activity

Epitope mapping indicated that six of the seven isolated mAbs recognized the EGF-like domain of human HB-EGF. This domain is essential for binding to and activation of EGFR (*31*). Thus we tested whether these mAbs have a neutralizing action on the signaling of HB-EGF to EGFR. To this end, DER cells, mouse hematopoietic 32D cells exogenously expressing EGFR (*5*), were cultured with rhHB-EGF (10 ng/ml) in the presence of each mAb or CRM197, which is a non-toxic mutant of DT that specifically binds to and neutralizes HB-EGF (*27*), at several concentrations. Since the mitogenic activity of HB-EGF and the inhibitory activity of CRM197 for HB-EGF are both up-regulated by heparin (*30*, *32*), assays were carried out in the presence or absence of heparin (10 μg/ml). As shown in Fig. 7, growth of DER cells in the presence of heparin was ~30% higher than in heparin-free conditions without inhibitors. Anti-HB-EGF neutralizing pAb strongly inhibited HB-EGF-mediated DER cell growth independently of heparin, while CRM197 and MAB259 inhibited DER cell growth more in the presence of heparin than without heparin. However, none of the seven new mAbs exhibited any inhibitory activity on the mitogenic activity of HB-EGF even in the presence of heparin. Thus, the mAbs isolated in this study are not useful for neutralization of HB-EGF mitogenic activity, at least in this assay, although except for 6C11 they all recognized the EGF-like domain.

Inhibition of DT binding to HB-EGF

DT binds to the EGF-like domain of HB-EGF (*27*, *28*). Especially, E141 is an important region for DT-binding in the EGF-like domain (*28*). Thus, we investigated whether mAbs inhibit the binding of DT to HB-EGF. Among all the mAbs, 4G10, 1F3 and 5D9 in the E141-group, 7E10 in the I133/H135-group and MAB259 in the H135-group were selected for this test. Vero-H cells were incubated with ^{125}I-labelled DT (50 ng/ml) and each mAb at various concentrations of mAb. All the mAbs tested inhibited the binding of DT to HB-EGF to the surface of Vero-H cells (Fig. 8) regardless of their recognizing region of the EGF-like domain.

Inhibition of HB-EGF ectodomain shedding

sHB-EGF, which is a potent mitogen and chemoattractant, is derived from proHB-EGF by ectodomain shedding. Thus, this process is critical for HB-EGF molecular function. For ectodomain shedding, proteases react with the juxtamembrane domain of HB-EGF, which is located just under the EGF-like domain, raising the possibility that anti-HB-EGF mAbs may inhibit the ectodomain shedding. Thus we investigated whether mAbs also inhibit this process.

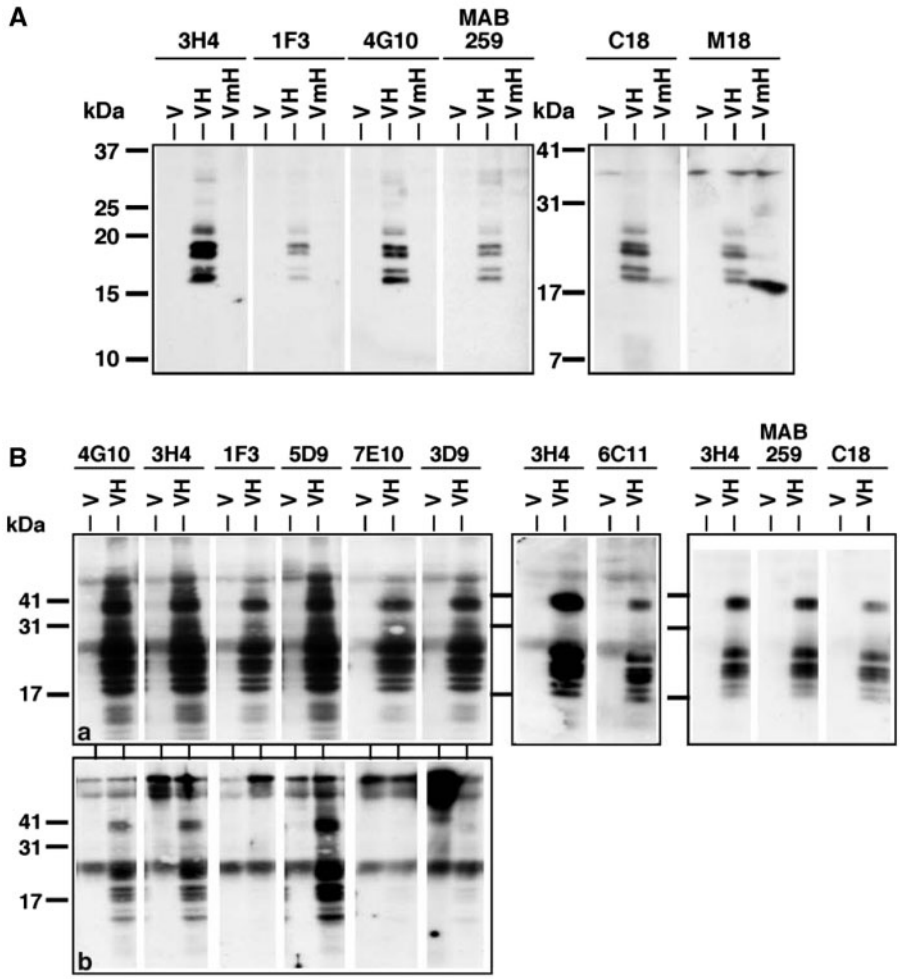

Fig. 5 Immunoblotting and immunoprecipitation assay. (A) Each mAb was tested for immunoblotting against lysates of Vero (V), Vero-H (VH) or Vero-mH (VmH) cells. 3H4 and 4G10 strongly; and 1F3 and MAB259 weakly detected human HB-EGF. Anti-human HB-EGF pAb C-18 (C18) and anti-mouse HB-EGF pAb M-18 (M18) were used for confirmation of human HB-EGF expression in Vero-H cells and mouse HB-EGF expression in Vero-mH cells. (B) Immunoprecipitation assay. Cell surfaces of Vero (V) and Vero-H (VH) cells were labelled by biotin, and cell lysates were immunoprecipitated with each mAb (2 and 0.1 μg/ml in a and b, respectively). All mAbs detected human HB-EGF. Anti-human HB-EGF pAb C-18 (C18) was used for confirmation of human HB-EGF expression in Vero-H cells.

TPA is a strong shedding-inducer for HB-EGF (*8*). As shown in Fig. 9A and B, all tested mAbs more or less inhibited TPA-induced HB-EGF shedding. Among them, the inhibitory activities of 4G10, 3H4 and 1F3 in the E141-group were relatively stronger than those of the other mAbs in the other epitope groups.

We then tested whether the shedding inhibitory activity of mAbs depends on the difference between the shedding inducers. LPA and anisomycin also induce HB-EGF shedding via distinct signaling pathways (the ERK- and p38MAPK-pathway, respectively), while TPA induces shedding via the PKC-pathway (*33–35*). As shown in Fig. 9C, all tested mAbs inhibited LPA- and anisomycin-induced HB-EGF shedding to a similar degree as TPA-induced shedding. These results suggest that recognition of E141 by a mAb is important for the inhibition of HB-EGF shedding. Consistently, CRM197, a non-toxic mutant of DT primarily requiring E141 for binding to HB-EGF, also strongly inhibited the shedding by all inducers.

To confirm that the shedding inhibitory activity of mAbs requires binding to HB-EGF, Vero-mH cells were tested for the shedding inhibition assay. All the mAbs obtained in this study were bound to human HB-EGF, but not to mouse HB-EGF (Fig. 2). None of the mAbs inhibited the ectodomain shedding of mouse HB-EGF, though the mAbs strongly inhibited the ectodomain shedding of human HB-EGF in the parallel experiment (Fig. 10A). In addition, the mAbs did not inhibit the ectodomain shedding of the other EGFR ligands (TGFα and EPR) (Fig. 10B). These results suggest that the HB-EGF shedding inhibitory activity of mAbs requires binding to HB-EGF.

Inhibition of ectodomain shedding-dependent cell growth

Inhibition of ectodomain shedding by mAbs should result in suppression of cell growth in an autocrine or paracrine growth model. To demonstrate this possibility, we examined the growth inhibitory activity of

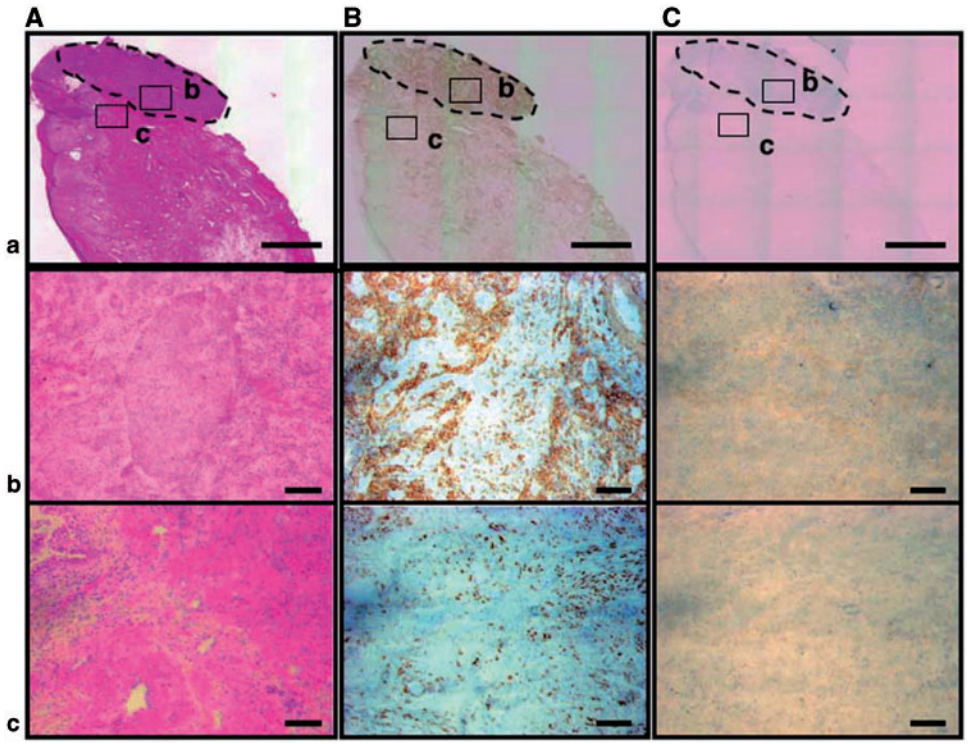

Fig. 6 Immunohistochemistry for cervical cancer tissues. Frozen sections of human cervical cancer tissues were stained with haematoxylin-eosin (A), mAb 5D9 (B) or the secondary antibody only (C). Magnifications of the sections indicated by rectangles in the figures of the top row a are shown in rows b (cancerous tissue, indicated by dashed lines) and c (non-cancerous tissue). Brown grains are positive for staining with mAb 5D9, and are observed abundantly in the mesenchymal area surrounding the cancer cells in cancerous regions (B-b). Bars: 2 mm for a, and 0.1 mm for b and c.

the mAbs through the inhibition of proHB-EGF ectodomain shedding by a bioassay in which DER cells were co-cultured with Vero-H cells under separation with Transwell inserts in the presence or absence of the mAb. Under these conditions DER cells can grow on HB-EGF secreted from Vero-H cells by ectodomain shedding. Heparin (10 μg/ml) was also added to all test samples to avoid loss of HB-EGF in the conditioned medium through the binding onto the surface of Vero-H cells via interaction with heparan–sulphate (*30*). Although none of the seven new mAbs exhibited any direct inhibition of the mitogenic activity of HB-EGF to DER cells (Fig. 7), mAbs 4G10, 3H4 and 1F3, which have strong inhibitory activities for shedding, significantly inhibited DER cell growth (Fig. 11). Expectedly, CRM197, inhibiting both the mitogenic activity and the shedding of HB-EGF, most strongly inhibited DER cell growth. MAB259 and Neut pAb, which strongly inhibit the mitogenic activity but have little to no effect on shedding, inhibited DER cell growth. 6C11, which only has moderate shedding inhibitory activity, did not significantly inhibit DER cell growth (Fig. 10). These results indicate that the new mAbs can inhibit cell growth mediated by HB-EGF in a paracrine manner through the inhibition of ectodomain shedding, but not through direct neutralization of HB-EGF mitogenic activity.

Discussion

MAbs could be important tools for various research purposes. However, few mAbs reacting with HB-EGF have been established to date. In this study, we immunized HB-EGF null mice with a recombinant human HB-EGF protein and established seven hybridoma clones producing mAbs that recognize human HB-EGF. The epitopes in the HB-EGF molecule that were recognized by these mAbs were mapped, and the applicability of each mAb for several research applications was examined. We also showed that some of the mAbs inhibited ectodomain shedding of proHB-EGF, resulting in suppression of cell growth in a co-culture assay system. Employment of these mAbs in research applications combined with the information provided by epitope mapping will further progress the research on HB-EGF.

Isolation of the anti-human HB-EGF mAbs for various research applications

In our precedent studies to obtain mAbs to HB-EGF by conventional immunization using wild-type mice we failed to raise any anti-human HB-EGF mAbs. We suspected that this might be caused by the high homology between the human and mouse HB-EGF proteins, and that immunization of HB-EGF null mice with the HB-EGF protein may facilitate the establishment of mAbs to HB-EGF. As shown in this study, we obtained seven different mAbs to human HB-EGF by immunization of HB-EGF null mice. However, all the mAbs isolated in this study reacted to human HB-EGF but not to mouse HB-EGF, indicating that no antibodies reacting with common epitopes of human and mouse HB-EGF were obtained by this immunization. Thus, further studies are required to verify the

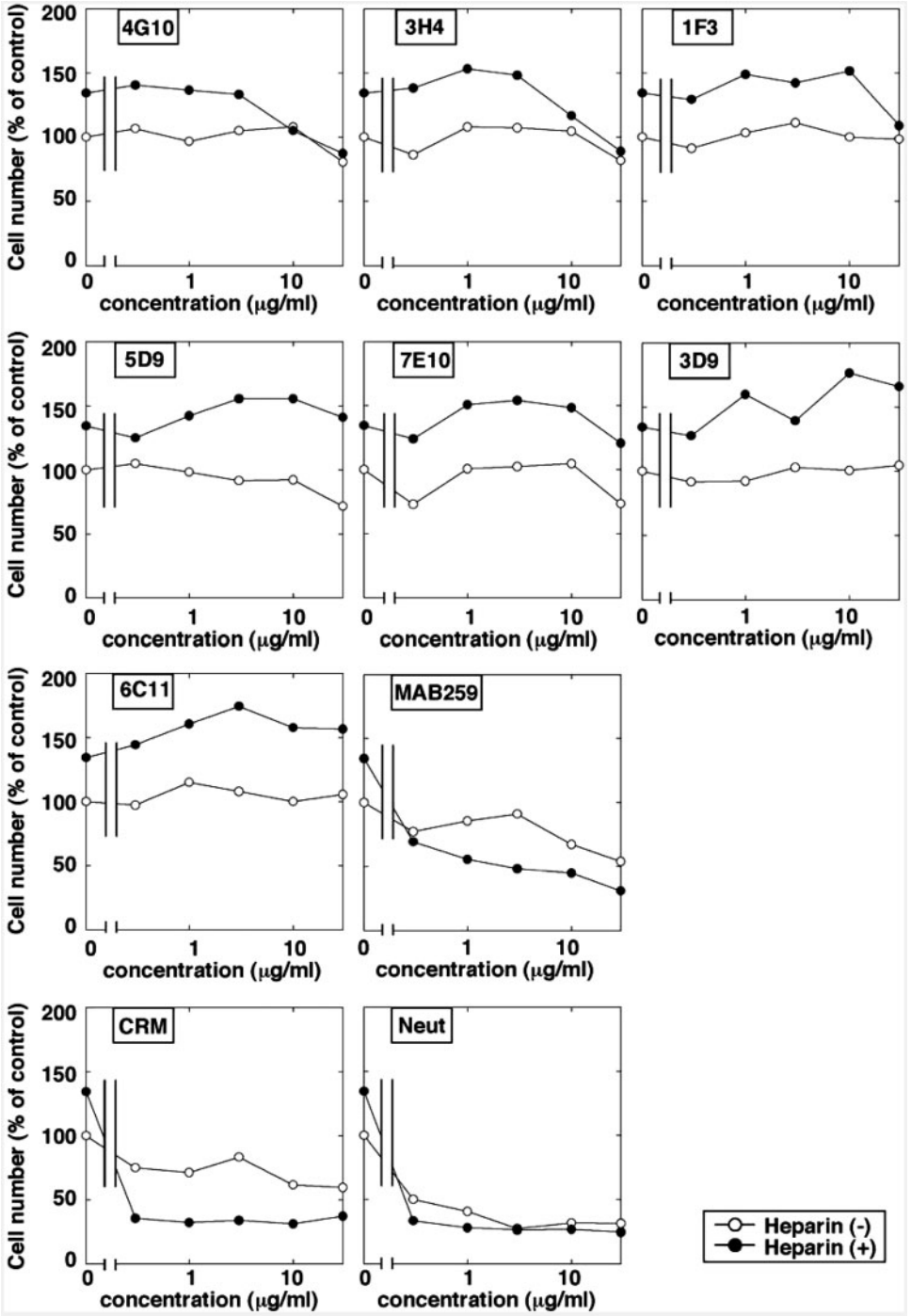

Fig. 7 Effect of each mAb on the mitogenic activity of human HB-EGF. DER cells were incubated with rhHB-EGF (10 ng/ml) and various concentrations of each mAb in the presence (solid circles) or absence (open circles) of heparin (10 μg/ml) for 42 h. Cell number was measured by MTT assay as described in the 'Materials and Methods' section, and expressed as the percentage of the mean score of samples without inhibitors and heparin.

advantage of the use of HB-EGF null mice for raising anti-HB-EGF antibodies.

In this study, the suitability of each mAb for several research applications was evaluated (summarized in Table I). For cell binding, 4G10, 3H4, 1F3, 7E10 and 3D9 had higher activities, even at the concentration of 0.1 μg/ml (Fig. 2), showing suitability for cell staining. We confirmed that these mAbs do indeed clearly stain HB-EGF on the cell surface (data not shown). For immunoblotting, 4G10 and 3H4 had higher activities (Fig. 5A). However, it should be noted that these mAbs could not work for samples subjected by SDS–PAGE in a reducing condition. For immunoprecipitation, 4G10, 3H4 and 5D9 had higher activities, even at the concentration of 0.1 μg/ml (Fig. 5B). For immunohistochemistry,

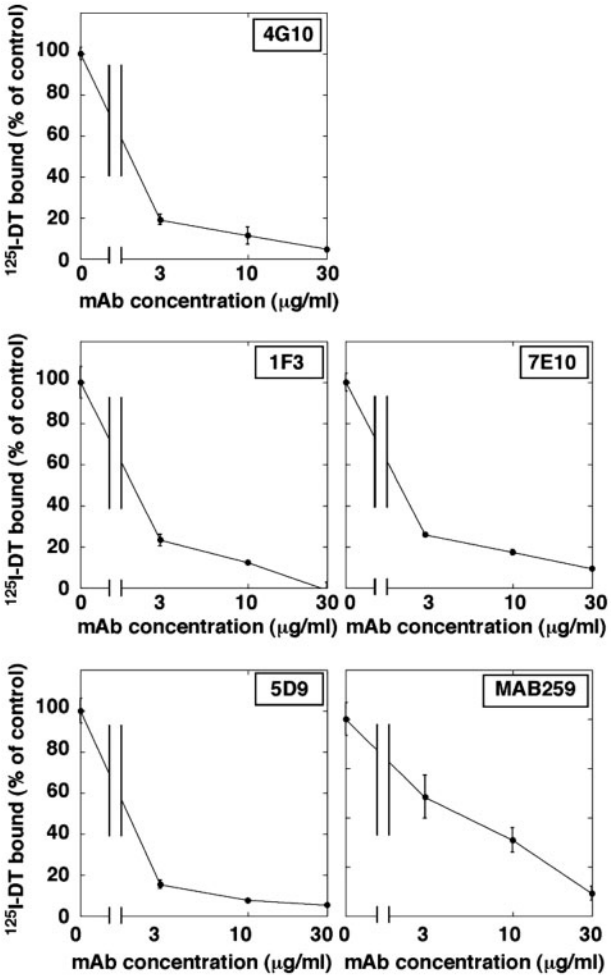

Fig. 8 Inhibition of DT binding to human HB-EGF by each mAb. Vero-H cells were incubated with ^{125}I-labelled DT (50 ng/ml) and various concentrations of each mAb for 12 h at 4°C, and the specific binding of the labelled DT was measured. The data are expressed as a percentage of the specific binding to the control without mAb. Each plot indicates the mean ± SE ($n = 3$).

5D9 (as well as MAB259) had the best results of the seven mAbs studied (Fig. 6). Regarding inhibition of HB-EGF bioactivities, the DT-binding activity of HB-EGF on the cell surface was strongly inhibited by all mAbs tested (Fig. 8), while the mitogenic activity of sHB-EGF was scarcely inhibited by any mAb isolated in this study (Fig. 7).

Inhibition of ectodomain shedding of proHB-EGF

We have shown that the isolated mAbs 4G10, 1F3 and 3H4 strongly suppressed the ectodomain shedding of proHB-EGF, while MAB259 or anti-HB-EGF neutralizing pAb showed week inhibitory activity (Fig. 9). This is the first observation that molecule binding to HB-EGF, such as mAbs, inhibits the ectodomain shedding of proHB-EGF. We also demonstrated that these mAbs inhibited cell growth of DER cells in a co-culture system by inhibiting the release of sHB-EGF from proHB-EGF-expressing Vero-H cells (Fig. 11), although these mAbs did not show any inhibitory activity on the soluble form of HB-EGF directly (Fig. 7). Ectodomain shedding of proHB-EGF is strongly inhibited by hydroxamic acid-based metalloprotease inhibitors (*8*, *33*). These metalloprotease inhibitors are powerful tools for proving the involvement of ectodomain shedding in biological phenomena, as they broadly inhibit metalloproteases and thus prevent ectodomain-shedding of many membrane proteins. Since the anti-HB-EGF mAbs isolated in this study specifically bind to HB-EGF, these mAbs may be used as HB-EGF-specific ectodomain-shedding inhibitors.

CRM197, a mutant form of DT, has long been recognized to be a non-toxic protein (*26*, *36*) that binds to HB-EGF and inhibits the mitogenic activity of HB-EGF by blocking the mitogenic activity of sHB-EGF (*27*). CRM197 strongly inhibits tumour growth in nude mice and thus the development of CRM197 for the treatment of ovarian and other cancers is now underway (*24*, *25*). In our previous study we demonstrated CRM197 still has a weak toxicity, though the toxicity of CRM197 is $\sim 10^6$ times less than that of wild-type DT (*37*). Thus, the inhibitory effect of CRM197 on cancer cell growth is expected to be caused by a cytotoxic effect on cancer cells expressing a high level of proHB-EGF, in addition to blocking the mitogenic activity of sHB-EGF. In the present study, we demonstrated that CRM197 effectively inhibited ectodomain shedding of proHB-EGF. This may contribute to the inhibitory effect of CRM197 on cancer cell growth.

Relationship between the inhibitory activities and the epitopes of mAbs

In the cell binding assay, all mAbs bound to human HB-EGF, but not to mouse HB-EGF. Utilizing this species specificity, we performed epitope mapping of each mAb. As a result, most of the mAbs (six out of seven) recognized the EGF-like domain, and mAbs recognizing the EGF-like domain were further sub-divided to three epitope groups: the E141-group (4G10, 3H4, 1F3 and 5D9), the H135-group (MAB259) and the I133/H135-group (7E10 and 3D9). In the inhibition assay for the HB-EGF mitogenic activity to DER cells, none of our mAbs had apparent inhibitory activities (Fig. 7). Conversely, in the inhibition assay for DT-binding, all mAbs tested so far had apparent inhibitory activities (Fig. 8). Thus, we could not detect any functional relationships between the inhibitory activities and the recognizing regions of HB-EGF by mAbs in these assays. Interestingly, however, the results of the inhibition assay for the HB-EGF ectodomain shedding showed some relationships among the recognizing regions. Among all tested mAbs, the inhibitory activity of 4G10, 3H4 and 1F3 in the E141-group was stronger than those of the other mAbs in the other epitope groups, regardless of the different shedding inducing stimuli such as TPA, LPA and anisomycin. CRM197 also strongly inhibited the shedding by all inducers. It has been known that E141 is a most critical amino acid for the binding of CRM197 and DT to HB-EGF (*28*, *38*). These results suggest that binding of E141 and the surrounding regions by mAb or CRM197 is important for the

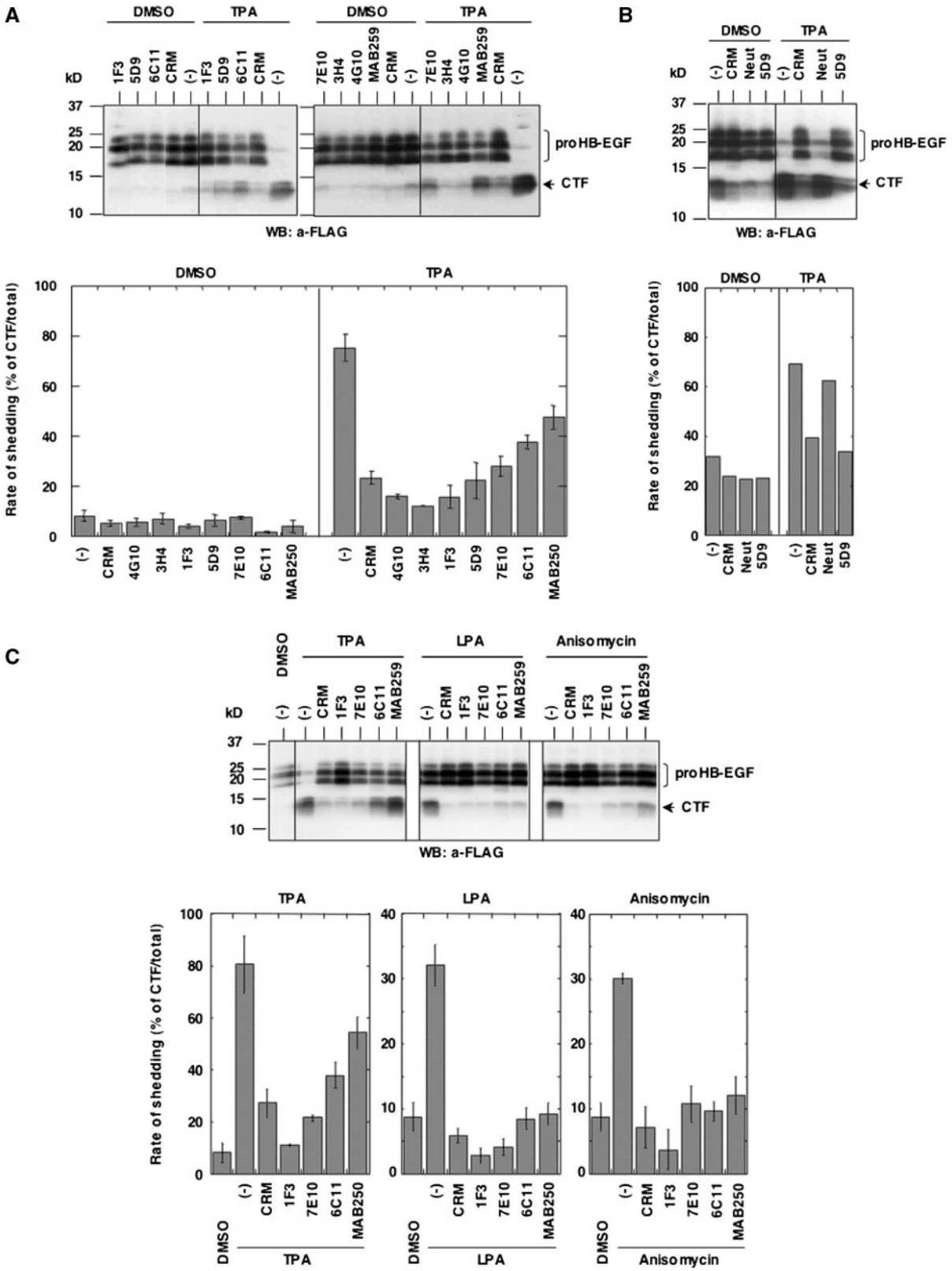

Fig. 9 Effect of each mAb on the ectodomain shedding of human HB-EGF. (A and B) Vero-H-FLAG cells were untreated (−) or pretreated with indicated mAb, neutralizing pAb (Neut) or CRM197, and then stimulated by TPA or DMSO only. TPA-induced HB-EGF shedding was monitored by immunoblotting using an anti-FLAG antibody (upper panel). Quantification of the extent of shedding was performed by densitometry, and calculated as the ratio of the density of the C-terminal fragment to that of the total band (lower panel). Each bar indicates the mean ± SE ($n = 3$). (C) Vero-H-FLAG cells were pretreated with the indicated mAb or CRM197, and then stimulated by TPA, LPA, or anisomycin. HB-EGF shedding was monitored by immunoblotting using an anti-FLAG antibody (upper panel). Quantification of the extent of shedding was performed by densitometry, and calculated as the ratio of the density of the C-terminal fragment to that of the total band (lower panel). Each bar indicates the mean ± SE ($n = 3$).

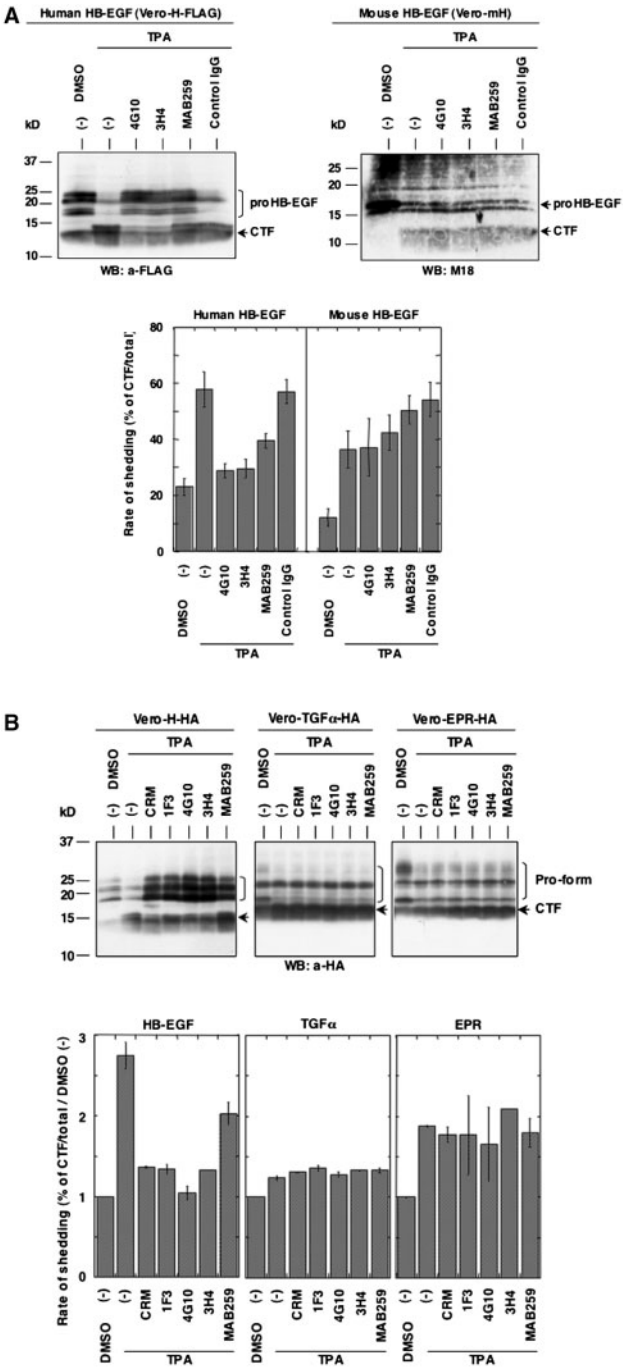

Fig. 10 Specificity of the shedding inhibitory activity of mAbs. (A) Vero-H-FLAG and Vero-mH cells were untreated (−) or pretreated with indicated mAb, and then stimulated by TPA or DMSO only. TPA-induced HB-EGF shedding was monitored by immunoblotting using an anti-FLAG antibody and M-18 antibody for human HB-EGF and mouse HB-EGF, respectively (upper panel). Quantification of the extent of shedding was performed by densitometry, and calculated as the ratio of the density of the C-terminal fragment to that of the total band (lower panel). Each bar indicates the mean ± SE ($n = 3$). (B) Vero-H-HA, Vero-TGFα-HA and Vero-EPR-HA cells were pretreated with the indicated mAb or CRM197, and then stimulated by TPA or DMSO only. TPA-induced shedding of HB-EGF, TGFα or EPR was monitored by immunoblotting using an anti-HA antibody (upper panel). Quantification of the extent of shedding was performed by densitometry and calculated as the ratio of the density of the C-terminal fragment to that of the total band (lower panel). Each bar indicates the mean ± SE ($n = 3$).

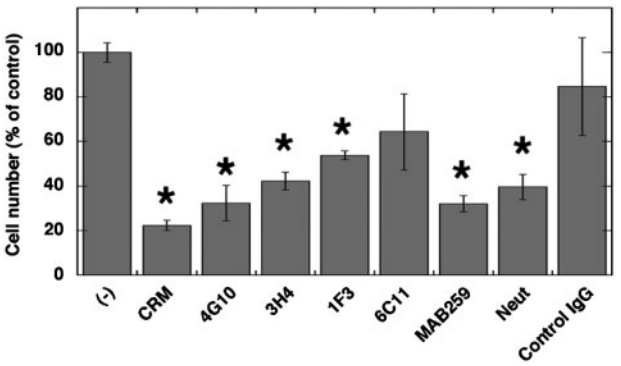

Fig. 11 Inhibition of DER cell growth co-cultured with Vero-H cells by inhibiting ectodomain shedding of proHB-EGF. DER cells were co-cultured with Vero-H cells under separation with Transwell inserts in the absence (−) or presence of 10 μg/ml anti-HB-EGF mAb, neutralizing pAb (Neut) or CRM197 for 48 h. The number of DER cells in the Transwell was measured as described in the 'Materials and Methods' section, and indicated as a percentage of the mean score of samples without inhibitors. Each bar represents the mean ± SE ($n = 3$). *$P < 0.01$.

inhibition of HB-EGF shedding by metalloproteases. However, further studies will be needed to carefully rule out the possibility that the difference in shedding inhibitory activity is due to the difference of affinity for HB-EGF.

Acknowledgements

The authors thank I. Ishimatsu for technical assistance in immunohistochemistry.

Funding

Grant-in-Aid from the Ministry of Education, Culture, Sports, Science, and Technology (17014057 and 18370079 for E.M.).

Conflict of interest

None declared.

References

1. Elenius, K., Paul, S., Allison, G., Sun, J., and Klagsbrun, M. (1997) Activation of HER4 by heparin-binding EGF-like growth factor stimulates chemotaxis but not proliferation. *EMBO J.* **16**, 1268–1278
2. Higashiyama, S., Abraham, J.A., Miller, J., Fiddes, J.C., and Klagsbrun, M. (1991) A heparin-binding growth factor secreted by macrophage-like cells that is related to EGF. *Science* **251**, 936–939
3. Higashiyama, S., Lau, K., Besner, G.E., Abraham, J.A., and Klagsbrun, M. (1992) Structure of heparin-binding EGF-like growth factor. Multiple forms, primary structure, and glycosylation of the mature protein. *J. Biol. Chem.* **267**, 6205–6212
4. Higashiyama, S., Iwamoto, R., Goishi, K., Raab, G., Taniguchi, N., Klagsbrun, M., and Mekada, E. (1995) The membrane protein CD9/DRAP 27 potentiates the juxtacrine growth factor activity of the membrane-anchored heparin-binding EGF-like growth factor. *J. Cell Biol.* **128**, 929–938
5. Iwamoto, R., Handa, K., and Mekada, E. (1999) Contact-dependent growth inhibition and apoptosis of epidermal growth factor (EGF) receptor-expressing

cells by the membrane-anchored form of heparin-binding EGF-like growth factor. *J. Biol. Chem.* **274**, 25906–25912
6. Iwamoto, R., Higashiyama, S., Mitamura, T., Taniguchi, N., Klagsbrun, M., and Mekada, E. (1994) Heparin-binding EGF-like growth factor, which acts as the diphtheria toxin receptor, forms a complex with membrane protein DRAP27/CD9, which up-regulates functional receptors and diphtheria toxin sensitivity. *EMBO J.* **13**, 2322–2330
7. Naglich, J.G., Metherall, J.E., Russell, D.W., and Eidels, L. (1992) Expression cloning of a diphtheria toxin receptor: identity with a heparin-binding EGF-like growth factor precursor. *Cell* **69**, 1051–1061
8. Goishi, K., Higashiyama, S., Klagsbrun, M., Nakano, N., Umata, T., Ishikawa, M., Mekada, E., and Taniguchi, N. (1995) Phorbol ester induces the rapid processing of cell surface heparin-binding EGF-like growth factor: conversion from juxtacrine to paracrine growth factor activity. *Mol. Biol. Cell.* **6**, 967–980
9. Raab, G. and Klagsbrun, M. (1997) Heparin-binding EGF-like growth factor. *Biochim. Biophys. Acta.* **1333**, F179–199
10. Mekada, E. and Iwamoto, R. (2008) HB-EGF. *UCSD-Nature Molecule Pages*. doi:10.1038/mp.a002932.01
11. Iwamoto, R. and Mekada, E. (2006) ErbB and HB-EGF signaling in heart development and function. *Cell Struct. Funct.* **31**, 1–14
12. Iwamoto, R., Yamazaki, S., Asakura, M., Takashima, S., Hasuwa, H., Miyado, K., Adachi, S., Kitakaze, M., Hashimoto, K., Raab, G., Nanba, D., Higashiyama, S., Hori, M., Klagsbrun, M., and Mekada, E. (2003) Heparin-binding EGF-like growth factor and ErbB signaling is essential for heart function. *Proc. Natl Acad. Sci. USA* **100**, 3221–3226
13. Jackson, L.F., Qiu, T.H., Sunnarborg, S.W., Chang, A., Zhang, C., Patterson, C., and Lee, D.C. (2003) Defective valvulogenesis in HB-EGF and TACE-null mice is associated with aberrant BMP signaling. *EMBO J.* **22**, 2704–2716
14. Yamazaki, S., Iwamoto, R., Saeki, K., Asakura, M., Takashima, S., Yamazaki, A., Kimura, R., Mizushima, H., Moribe, H., Higashiyama, S., Endoh, M., Kaneda, Y., Takagi, S., Itami, S., Takeda, N., Yamada, G., and Mekada, E. (2003) Mice with defects in HB-EGF ectodomain shedding show severe developmental abnormalities. *J. Cell Biol.* **163**, 469–475
15. Mine, N., Iwamoto, R., and Mekada, E. (2005) HB-EGF promotes epithelial cell migration in eyelid development. *Development* **132**, 4317–4326
16. Shirakata, Y., Kimura, R., Nanba, D., Iwamoto, R., Tokumaru, S., Morimoto, C., Yokota, K., Nakamura, M., Sayama, K., Mekada, E., Higashiyama, S., and Hashimoto, K. (2005) Heparin-binding EGF-like growth factor accelerates keratinocyte migration and skin wound healing. *J. Cell Sci.* **118**, 2363–2370
17. Kimura, R., Iwamoto, R., and Mekada, E. (2005) Soluble form of heparin-binding EGF-like growth factor contributes to retinoic acid-induced epidermal hyperplasia. *Cell Struct. Funct.* **30**, 35–42
18. Xie, H., Wang, H., Tranguch, S., Iwamoto, R., Mekada, E., Demayo, F.J., Lydon, J.P., Das, S.K., and Dey, S.K. (2007) Maternal heparin-binding-EGF deficiency limits pregnancy success in mice. *Proc. Natl Acad. Sci. USA* **104**, 18315–18320
19. Minami, S., Iwamoto, R., and Mekada, E. (2008) HB-EGF decelerates cell proliferation synergistically with TGFalpha in perinatal distal lung development. *Dev. Dyn.* **237**, 247–258
20. Asakura, M., Kitakaze, M., Takashima, S., Liao, Y., Ishikura, F., Yoshinaka, T., Ohmoto, H., Node, K., Yoshino, K., Ishiguro, H., Asanuma, H., Sanada, S., Matsumura, Y., Takeda, H., Beppu, S., Tada, M., Hori, M., and Higashiyama, S. (2002) Cardiac hypertrophy is inhibited by antagonism of ADAM12 processing of HB-EGF: metalloproteinase inhibitors as a new therapy. *Nat. Med.* **8**, 35–40
21. Miyagawa, J., Higashiyama, S., Kawata, S., Inui, Y., Tamura, S., Yamamoto, K., Nishida, M., Nakamura, T., Yamashita, S., Matsuzawa, Y., and Taniguchi, N. (1995) Localization of heparin-binding EGF-like growth factor in the smooth muscle cells and macrophages of human atherosclerotic plaques. *J. Clin. Invest.* **95**, 404–411
22. Powell, P.P., Klagsbrun, M., Abraham, J.A., and Jones, R.C. (1993) Eosinophils expressing heparin-binding EGF-like growth factor mRNA localize around lung microvessels in pulmonary hypertension. *Am. J. Pathol.* **143**, 784–793
23. Fu, S., Bottoli, I., Goller, M., and Vogt, P.K. (1999) Heparin-binding epidermal growth factor-like growth factor, a v-Jun target gene, induces oncogenic transformation. *Proc. Natl. Acad. Sci. USA* **96**, 5716–5721
24. Miyamoto, S., Hirata, M., Yamazaki, A., Kageyama, T., Hasuwa, H., Mizushima, H., Tanaka, Y., Yagi, H., Sonoda, K., Kai, M., Kanoh, H., Nakano, H., and Mekada, E. (2004) Heparin-binding EGF-like growth factor is a promising target for ovarian cancer therapy. *Cancer Res.* **64**, 5720–5727
25. Miyamoto, S., Yagi, H., Yotsumoto, F., Kawarabayashi, T., and Mekada, E. (2006) Heparin-binding epidermal growth factor-like growth factor as a novel targeting molecule for cancer therapy. *Cancer Sci.* **97**, 341–347
26. Uchida, T., Pappenheimer, A.M.J., and Greany, R. (1973) Diphtheria toxin and related proteins. I. Isolation and some properties of mutant proteins serologically related to diphtheria toxin. *J. Biol. Chem.* **248**, 3838–3844
27. Mitamura, T., Higashiyama, S., Taniguchi, N., Klagsbrun, M., and Mekada, E. (1995) Diphtheria toxin binds to the epidermal growth factor (EGF)-like domain of human heparin-binding EGF-like growth factor/diphtheria toxin receptor and inhibits specifically its mitogenic activity. *J. Biol. Chem.* **270**, 1015–1019
28. Mitamura, T., Umata, T., Nakano, F., Shishido, Y., Toyoda, T., Itai, A., Kimura, H., and Mekada, E. (1997) Structure-function analysis of the diphtheria toxin receptor toxin binding site by site-directed mutagenesis. *J. Biol. Chem.* **272**, 27084–27090
29. Wang, X., Mizushima, H., Adachi, S., Ohishi, M., Iwamoto, R., and Mekada, E. (2006) Cytoplasmic domain phosphorylation of heparin-binding EGF-like growth factor. *Cell Struct. Funct.* **31**, 15–27
30. Takazaki, R., Shishido, Y., Iwamoto, R., and Mekada, E. (2004) Suppression of the biological activities of the epidermal growth factor (EGF)-like domain by the heparin-binding domain of heparin-binding EGF-like Growth Factor. *J. Biol. Chem.* **279**, 47335–47343
31. Harris, R.C., Chung, E., and Coffey, R.J. (2003) EGF receptor ligands. *Exp. Cell Res.* **284**, 2–13
32. Shishido, Y., Sharma, K.D., Higashiyama, S., Klagsbrun, M., and Mekada, E. (1995) Heparin-like molecules on the cell surface potentiate binding of diphtheria toxin to the diphtheria toxin receptor/membrane-anchored heparin-binding epidermal growth factor-like growth factor. *J. Biol. Chem.* **270**, 29578–29585

33. Izumi, Y., Hirata, M., Hasuwa, H., Iwamoto, R., Umata, T., Miyado, K., Tamai, Y., Kurisaki, T., Sehara-Fujisawa, A., Ohno, S., and Mekada, E. (1998) A metalloprotease-disintegrin, MDC9/meltrin-gamma/ADAM9 and PKCdelta are involved in TPA-induced ectodomain shedding of membrane-anchored heparin-binding EGF-like growth factor. *EMBO J.* **17**, 7260–7272
34. Takenobu, H., Yamazaki, A., Hirata, M., Umata, T., and Mekada, E. (2003) The stress- and inflammatory cytokine-induced ectodomain shedding of heparin-binding epidermal growth factor-like growth factor is mediated by p38 MAPK, distinct from the 12-O-tetradecanoylphorbol-13-acetate- and lysophosphatidic acid-induced signaling cascades. *J. Biol. Chem.* **278**, 17255–17262
35. Umata, T., Hirata, M., Takahashi, T., Ryu, F., Shida, S., Takahashi, Y., Tsuneoka, M., Miura, Y., Masuda, M., Horiguchi, Y., and Mekada, E. (2001) A dual signaling cascade that regulates the ectodomain shedding of heparin-binding epidermal growth factor-like growth factor. *J. Biol. Chem.* **276**, 30475–30482
36. Uchida, T., Gill, D.M., and Pappenheimer, A.M. Jr. (1971) Mutation in the structural gene for diphtheria toxin carried by temperate phage β. *Nature. New Biol.* **233**, 8–11
37. Kageyama, T., Ohishi, M., Miyamoto, S., Mizushima, H., Iwamoto, R., and Mekada, E. (2007) Diphtheria toxin mutant CRM197 possesses weak EF2-ADP-ribosyl activity that potentiates its anti-tumorigenic activity. *J. Biochem.* **142**, 95–104
38. Louie, G.V., Yang, W., Bowman, M.E., and Choe, S. (1997) Crystal structure of the complex of diphtheria toxin with an extracellular fragment of its receptor. *Mol. Cell.* **1**, 67–78